Picosecond Infrared Spectra of Isotope-Substituted 4-(Dimethylamino)benzonitriles and Molecular Structure of the Charge-Transfer Singlet Excited State

Hiromi Okamoto,*,†,‡ Hironori Inishi,§ Yuko Nakamura,§ Shigeru Kohtani,§ and Ryoichi Nakagaki§

Research Centre for Spectrochemistry, School of Science, The University of Tokyo, 7-3-1 Hongo, Bunkyo-ku, Tokyo 113-0033, Japan, and Faculty of Pharmaceutical Sciences, Kanazawa University, 13-1 Takara-machi, Kanazawa 920-0934, Japan

Received: October 25, 2000; In Final Form: February 2, 2001

Picosecond transient infrared spectra of 4-(dimethylamino)benzonitrile (DMABN) and several isotope-substituted samples have been recorded in the fingerprint region in acetonitrile solutions. Among several strong transient infrared bands of the intramolecular charge transfer (ICT) excited state, the band at 1276 cm^{-1} (for normal species) shifts to lower frequencies on ^{15}N, ^{13}C, and deuterium substitution of the dimethylamino group, and is assigned to the ring $C-NMe_2$ single-bond stretch. Other bands observed are attributable to vibrational modes of the benzonitrile moiety. The band frequencies obtained, together with those found in the literature, are compared with results of vibrational analyses based on CIS/6-31G level ab initio molecular orbital calculations. This treatment has made possible assignments of the bands due to the benzonitrile moiety. On the basis of the assignments, electronic structure of the ICT state is discussed. The electronic structure of the ICT state is suggested to be basically of benzenoid nature, with a significant contribution from quinoidal structure. An advanced theoretical treatment may be needed to obtain final conclusion on the structure (planar or twisted) of the ICT state.

1. Introduction

For nearly four decades, the 4-(dimethylamino)benzonitrile (DMABN) molecule has been well-known for its dual fluorescence behavior in polar solvents.[1−3] In nonpolar solvents, this molecule shows a single spectral component of fluorescence which is attributed to the locally excited (LE) state, whereas in polar solvent it shows another spectral component in the longer wavelength region, in addition to that due to the LE state. This red-shifted fluorescence is attributed to the intramolecular charge transfer (ICT) singlet excited state. On the molecular structure of the ICT state of DMABN, Grabowski and co-workers proposed a model of "twisted intramolecular charge transfer" (TICT), based on the fluorescence behavior of DMABN derivatives with restricted conformations of the dimethylamino group.[3−7] In this model, the dimethylamino group of DMABN is twisted perpendicularly to the benzene plane in the ICT state that charge recombination is hindered because of the "principle of minimum overlap". While this model has been widely accepted, various other structural models of the ICT state has been also discussed extensively. For example, from the systematic studies on substituent effects on fluorescence spectra of DMABN derivatives, it has been claimed that excited DMABN has a "planar intramolecular charge transfer" (PICT) structure, where all atoms except for the methyl-group hydrogens lie on the same plane.[8−11] Other structures of the ICT states have been discussed principally on the basis of theoretical calculations.[12−20] They include the "wagged intramolecular charge transfer" (WICT) model where the dimethylamino group is distorted to an out-of-plane direction to increase pyramidization of the amino nitrogen,[13,15,18] and the "rehybridized intramolecular charge transfer" (RICT) model where an in-plane bent geometry is considered for the cyano group structure.[16] In recent studies, it has been revealed that the RICT model cannot explain the observed infrared spectrum of the ICT state of DMABN,[19,21,22] and that the WICT model does not produce a highly polar state.[14,15,17,18,20] However, it has been still the subject of much controversy which one of TICT or PICT is more realistic for excited DMABN.[23,24]

On dynamic behavior of DMABN, it has been known, from time-resolved fluorescence and absorption data,[25−36] that the ICT state is generated on a time scale of several picoseconds to tens of picoseconds after photoexcitation in polar solvent. This state has a lifetime of hundreds of picoseconds. On the other hand, direct experimental evidence for the molecular structure of the ICT state of DMABN, other than experimental data on chemically modified compounds, has been very limited. Information on the structure of the ICT state is expected to be given by transient vibrational spectroscopy in the picosecond regime. Until recently, however, the picosecond transient infrared spectrum of the ICT state, especially in the fingerprint wavenumber region, was not measured because of experimental difficulties, and also the picosecond Raman spectrum was not observed for its strong fluorescence. The only vibrational spectrum of the ICT state in polar solvent was the nanosecond transient infrared spectrum in the C≡N triple bond stretching region,[37] but it was difficult to discuss the molecular structure only from this spectrum. As other approaches to the molecular structure of the ICT state, spectroscopic studies of DMABN-solvent complexes in a supersonic jet and those in supercritical fluid have been reported by several researchers.[38−46] However,

* Author to whom correspondence should be addressed. E-mail: aho@music.email.ne.jp.

† The University of Tokyo.

‡ Present address: Institute for Molecular Science, Myodaiji, Okazaki, Aichi 444-8585, Japan.

§ Kanazawa University.

10.1021/jp0039363 CCC: $20.00
Published on Web 04/06/2001

it is hardly said that much information on the geometrical structure of the excited DMABN itself has been obtained in these studies.

Recently, femto- to picosecond transient infrared[21,47] and Raman[48] spectra of the ICT state of DMABN have been reported by a few groups including us. Vibrational analyses based on CASSCF level ab initio molecular orbital calculation has been also reported for the TICT, PICT, and RICT structures.[22] However, the assignments of the observed infrared and Raman bands are not very clear. For clear vibrational assignments, spectral measurements on isotope-substituted samples are very informative. The unambiguous band assignments may be also important when we compare the observed spectra with vibrational frequencies calculated by the molecular orbital method, because it is not yet well established whether results of quantum-chemical vibrational calculations of excited molecules are accurate enough. For example, especially in the fingerprint region where cross terms of force fields have crucial effects on mode hybridization, it can be hardly said that the following points are examined sufficiently and systematically for a wide range of electronically excited species: whether quantum chemical calculations can predict the vibrational frequencies within tens of cm^{-1}, whether calculated infrared intensities are reliable, how selections of basis set and active space (for the CASSCF method) have effects on the result, and so on. In the present paper, we report picosecond transient infrared spectra of the ICT state of isotope-substituted DMABN. On the basis of the data obtained, with the aid of comparison with the related molecules and of molecular orbital calculations for some bands, we try to establish vibrational assignments of the observed infrared bands. We also discuss the electronic and molecular structure of the ICT state of DMABN.

2. Experimental Section

The experimental setup for the picosecond transient infrared spectroscopy in the fingerprint region was basically the same as that already reported elsewhere.[47,50,51] The essential points are briefly described here. The optical beams for the measurement was obtained from a synchronously pumped dye laser with a dye amplifier excited by the second harmonic output from a Nd:YLF regenerative amplifier. The repetition rate of the laser system was 1 kHz. The infrared probe beam in the wavenumber region between 1700 and 920 cm^{-1} was obtained by two-stage difference frequency mixing of the fundamental output (1053 nm) from the Nd:YLF regenerative amplifier and the output from the amplified dye laser. The ultraviolet pump beam was obtained as the second harmonic of the amplified dye laser (277−289 nm). The pump pulse energy was in the range between ca. 1 and 4 μJ. The cross correlation time of the pump and probe pulses was about 4 ps. The spectral resolution of the transient infrared spectra was about 8 cm^{-1}. In the present measurements delay time between the pump and probe pulses was fixed at 16 ps. At this delay time the excited DMABN relaxes for the most part to the ICT state, in the solvent adopted here (acetonitrile). We made use of a method based on optically heterodyned detection of absorption anisotropy (OHDAA),[51] in order to detect very small infrared absorbance change.

The isotopomers of DMABN measured in the present study were the natural ones (not isotope labeled), $Me_2N-C_6H_4-C^{15}N$ (abbreviated as $C^{15}N$), $Me_2{}^{15}N-C_6H_4-CN$ ($^{15}NMe_2$), $(^{13}CH_3)_2N-C_6H_4-CN$ ($^{13}C_2$), and $(CD_3)_2N-C_6H_4-CN$ (d_6). The method of preparing the isotope-substituted samples, the ground-state vibrational spectra, and analyses of them were described elsewhere.[52] The solvent (acetonitrile, liquid chromatography grade) was purchased from Wako Pure Chemicals and used as received. The concentration of the sample solution was $\sim 7 \times 10^{-2}$ mol dm^{-3}. The sample solution was circulated through a BaF_2 flow cell with an optical path length of 0.015 mm for the transient infrared measurements. The static infrared spectra of the ground-state molecules were measured for the same solutions by a JASCO FT/IR-420 Fourier transform infrared spectrophotometer.

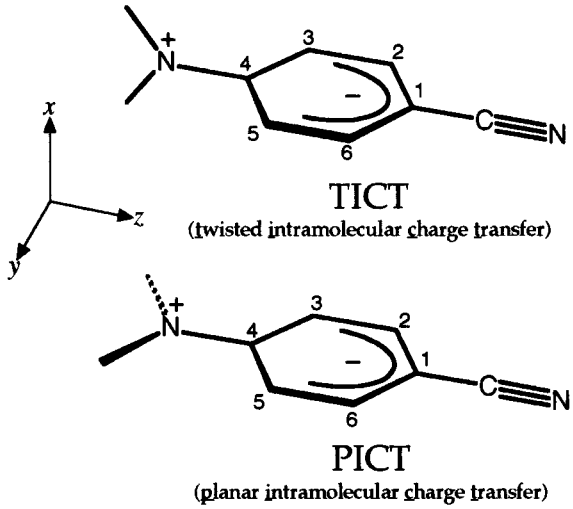

Figure 1. Possible molecular structures for the ICT state of DMABN.

3. Molecular Orbital Calculation

Geometry optimization and vibrational analysis based on ab initio molecular orbital calculation was performed, to obtain some insight into vibrational assignments. The calculation was done using the Gaussian 98 program[53] on a personal computer. The output of the program includes the intramolecular force field in Cartesian coordinate system. The force field in the Cartesian coordinate system was transformed into that in the symmetrized group coordinate system[52] by a homemade program, and then a normal coordinate calculation using this coordinate system was done. This treatment was needed to pick up dominant internal coordinates in a normal mode. Detail of the method was already described elsewhere for the vibrational analysis of the ground-state DMABN.[52] The molecular orbital calculations in CIS/6-31G(d) level were tried. We make use of the results of calculation only as a semiquantitative guide for vibrational assignments considering the crude calculation level. As for the molecular structure of the ICT state, we examined two possibilities (Figure 1): a structure having the coplanarity of the dimethylamino group with the benzonitrile moiety (corresponding to PICT) and a perpendicular conformation between the two moieties (corresponding to TICT). In both cases the molecular symmetries were assumed to belong to a C_{2v} point group.

4. Results

4.1. Observed Transient Infrared Spectra of Isotopomers of DMABN and Band Assignments. Static and transient infrared spectra of DMABN and isotopomers are shown in Figures 2 and 3, respectively. Delay time between the pump and probe pulses was 16 ps for the transient infrared measurements, and at this delay time the excited species is for the most part populated on the ICT state. In the wavenumber region measured, we have four strong induced infrared bands, all of which are found below 1430 cm^{-1}. No prominent band is

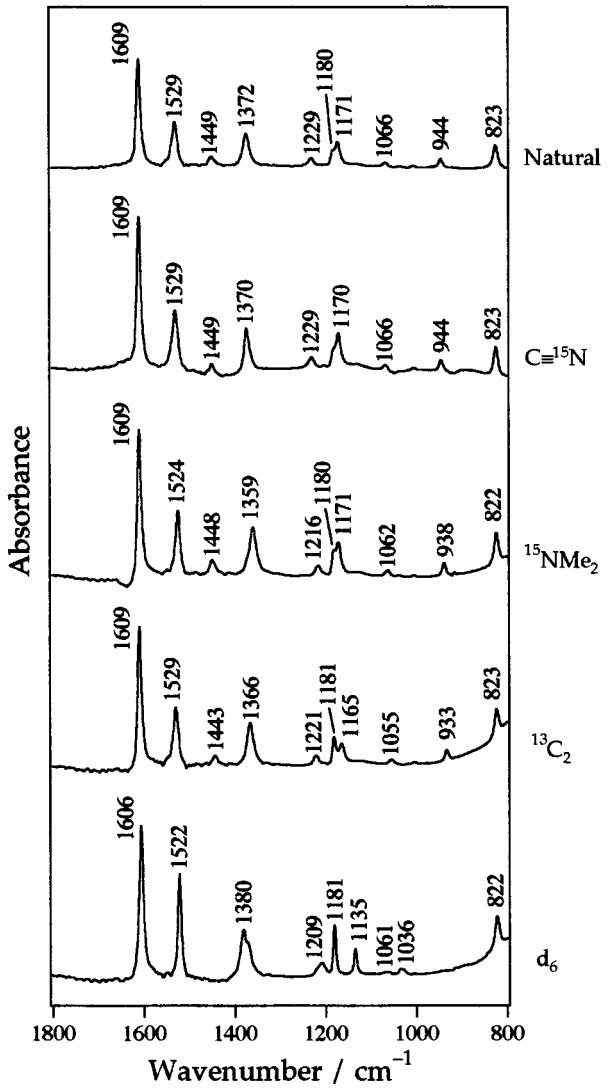

Figure 2. Static infrared spectra of DMABN and isotope-substituted species in acetonitrile solution. The solvent bands are numerically removed. The sample concentration is $\sim 7 \times 10^{-2}$ mol dm^{-3}.

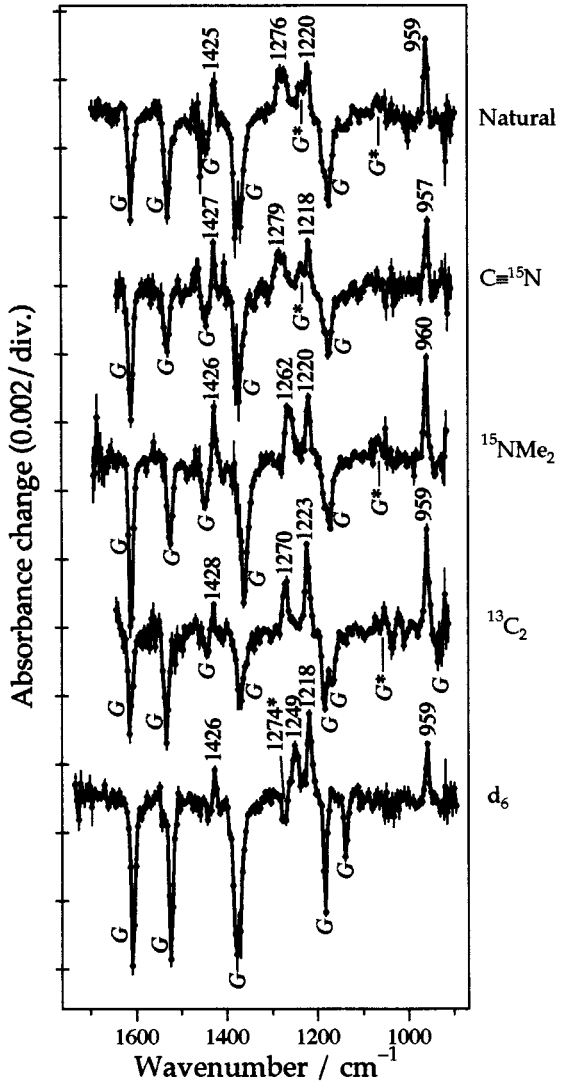

Figure 3. Transient infrared spectra of DMABN and isotope-substituted species in acetonitrile solution. The wavenumbers of bands attributed to the ICT state are given above each trace. The bands marked with "*G*" are due to the ground state. The asterisks represent the bands with negative signs. The sample concentration is $\sim 7 \times 10^{-2}$ mol dm^{-3}. Delay time between pump and probe pulses was 16 ps.

observed in the region higher than 1430 cm^{-1}. All of the four induced bands have positive (upper) absorption peaks. In the OHDAA method, an excited species gives a positive transient infrared absorption band when the angle between the electronic (for pumping) and vibrational (for probing) transition moments is smaller than 54.7°.[51] The direction of the electronic transition moment giving rise to the ultraviolet absorption around 280 nm is considered to be parallel to the long axis (*z*-axis under C_{2v} symmetry, which belongs to a_1 symmetry species) of the molecule. Accordingly, the vibrational transition moments of the positive transient infrared bands are also parallel to the long axis of the molecule. In other words, these bands can be attributed to totally symmetric vibrations under C_{2v} symmetry.

The C^{15}N species gives transient absorption bands at nearly the same positions as the natural DMABN. This situation is common to the infrared spectra of the ground-state species.[52] On the isotope substitutions of the dimethylamino group, on the other hand, the transient band at 1276 cm^{-1} of the normal species shifts toward lower wavenumbers. This observation, together with its vibrational frequency, clearly indicates that the band at 1276 cm^{-1} (normal species) is assigned to the mode with major contribution from the ring C−NMe$_2$ single bond stretch. Other transient bands do not show frequency shift on the isotope substitutions of the dimethylamino group, and are attributable to the modes of the benzonitrile moiety. One of the present authors (H.O.) presumed in the previous paper[47] that the C−NMe$_2$ stretch has a significant contribution to the band at ∼960 cm^{-1}, but this assignment should be abandoned.

In the d_6 species, we have obtained an interesting transient spectral pattern: the positive transient band of the normal species at 1276 cm^{-1} shifts to 1249 cm^{-1}, while there remains a negative transient band at 1274 cm^{-1}. When we carefully examine the transient infrared band of the normal species at 1276 cm^{-1}, we find that the band profile consists of two components, a strong positive band and a relatively weak negative band at almost the same peak position. Also in the other isotopomers, it seems that there are contributions of negative bands in the wavenumber region of 1280−1276 cm^{-1}. Since no prominent bands are observed in this wavenumber region in the ground-state infrared spectra, the negative band is considered to be an induced band of the ICT state. The negative band seems to show only very small (or no) shift on the isotope substitution of the dimethylamino group, in contrast to the positive band at 1276 cm^{-1} (normal species). The negative band is therefore assigned to a vibrational mode of the benzonitrile moiety. It is clear that the

vibrational transition moment of this band is perpendicular to the long axis of the molecule, from the negative sign of the band. It is hard to consider, from the band frequency, that this band is due to an out-of-plane vibration of the benzene ring. This band is then attributed to an in-plane nontotally symmetric (b_2 symmetry species) vibrational mode.

Recently, Chudoba et al. recorded the transient infrared spectrum of DMABN in acetonitrile (the same solvent as we have adopted) in femto- to picosecond regime.[21] They observed only one transient band of the ICT state at 2112 cm^{-1} which was assigned to the C≡N stretch. Hashimoto and Hamaguchi measured several years ago the nanosecond transient infrared spectrum of DMABN in butanol in the triple bond stretching region, and found a band attributable to the C≡N stretch of the singlet excited state at 2096 cm^{-1}.[37] Although the solvent adopted was different from that in the present study and the time scale was also different, the species observed was probably the identical ICT state. The frequencies of the C≡N stretching vibration in these two experimental reports are essentially the same, considering the difference in the solvent and the experimental errors.

Kwok et al. recently recorded a transient Raman spectrum of the ICT state of DMABN in methanol.[48] They utilized a new device to discriminate weak Raman scattering from strong fluorescence. Although the spectral quality does not seem to be very high in the present stage, the three prominent Raman peaks observed for the ICT state may be reliable. The observed Raman frequencies are 1585, 1182, and 946 cm^{-1}. Among them, the band 946 cm^{-1} is possibly attributable to the same vibrational mode as one giving rise to the transient infrared band at 959 cm^{-1} presently observed, considering that their spectral data have been obtained in each 10 cm^{-1} and that our solvent is different from that they have adopted. For the other two Raman bands (1585 and 1182 cm^{-1}), we have not observed any infrared bands at the corresponding positions. In the first column of Table 1, the band frequencies of the ICT state presently obtained are summarized, together with those so far reported by other groups.

4.2. Molecular Orbital Calculation. Bond lengths between heavy atoms (C and N) and dipole moments obtained by the geometry optimizations are summarized in Table 2. In Table 1, calculated vibrational frequencies corresponding to the observed ones are shown for the planar and twisted geometries together with their brief mode descriptions. The calculated frequencies have been scaled by the factors given in Table 1, which have been so obtained as to give the best fits to the observed frequencies.

In both of the calculation sets involved in Table 1, we have had relatively small imaginary frequencies of a_2 and/or b_1 symmetry species, but we continue the discussion here assuming C_{2v} symmetry. Generally, the geometry should be optimized. However, we treat the results of the CIS calculation only qualitatively in the present paper, and for this reason we perform the CIS calculation with the molecular symmetry restricted to C_{2v}.

In Table 2, the calculated dipole moment for the planar geometry seems to be too small compared with that based on the more sophisticated CASSCF method.[22] Similarly, the calculated C−NMe_2 bond length for the twisted geometry may be too short. These results show difficulties in quantitative discussion on the basis of the CIS calculations.[19,22] We therefore use the results of the CIS calculations only for qualitative or semiquantitative guides for the vibrational assignments of principally the ring mode.

TABLE 1: Observed and Calculated Vibrational Frequencies (in cm^{-1}) and Assignments of the ICT State of DMABN and Isotopomers[a]

	CIS/6-31G(d)[b]		
obs.	planar	twisted	assignment
	Natural		
2096[c], 2112[d]	2035	2246	C≡N
	C≡N	C≡N	
1585[e]	1559	1576	8a
	8a	8a	
1425	1425	1357	19a
	19a	19a	
1276	1350	1379	4-N
	4-N,18a	4-N	
1276	1316	1306	3 or 14
	3	3	
1220	1183	1185	1-C
	1-C	1-C	
1182[e]	1134	1138	9a
	9a	9a	
959, 946[e]	919	922	12
	12	12	
	$^{15}NMe_2$		
1426	1420	1354	19a
	19a	19a	
1280	1316	1306	3 or 14
	3	3	
1262	1337	1366	4-N
	4-N,18a	4-N	
1220	1183	1185	1-C
	1-C	1-C	
960	917	922	12
	12	12	
	$^{13}C_2$		
1428	1420	1357	19a
	19a	19a	
1270	1346	1376	4-N
	4-N,18a	4-N	
1223	1183	1185	1-C
	1-C	1-C	
959	916	922	12
	12	12	
	d_6		
1426	1430	1360	19a
	19a	19a	
1274	1319	1306	3 or 14
	3	3	
1249	1342	1369	4-N
	4-N,18a	4-N	
1218	1184	1184	1-C
	1-C	1-C	
959	904	916	12
	12,19a	12,19a	
scale factor	0.879	0.887	

[a] Infrared band frequencies observed for the C≡^{15}N species are essentially the same as those of the natural one and not listed in this table. Abbreviations for the intramolecular coordinates: C≡N, C≡N stretch; 4-N, ring C−NMe_2 stretch; Nsc, NMe_2 scissors; 1-C, ring C−CN stretch; 8a, 19a, 18a, 3, 14, 9a, 12, and 6a, Wilson notations of benzene ring modes.[54] [b] The assignment of the mode for each calculation is given below the frequency. [c] Hashimoto and Hamaguchi,[34] nanosecond infrared band in butanol. [d] Chudoba et al.,[21] femtosecond infrared band in acetonitrile. [e] Kwok et al.,[48] picosecond Raman band in methanol.

5. Discussion

5.1. Assignments of the Observed Vibrational Bands of the ICT State. In the previous section, the transient band at 1276 cm^{-1} (normal species) has been assigned to the mode with major contribution from the C−NMe_2 single bond stretch, on

TABLE 2: Calculated Bond Distances (in Å) and Dipole Moments (in Debye) for the ICT State of DMABN

	CIS/6-31G(d)		Dreyer, Kummrow[b]	
bond[a]	planar	twisted	PICT	TICT
4−N	1.366	1.342	1.351	1.433
4−3, 4−5	1.443	1.465	1.438	1.423
3−2, 5−6	1.357	1.353	1.385	1.361
2−1, 6−1	1.443	1.415	1.448	1.429
1−CN	1.402	1.421	1.402	1.417
C≡N	1.153	1.143	1.151	1.145
N−Me	1.446	1.455	1.453	1.457
dipole moment	9.1	13.7	13.1	15.6

[a] See Figure 1 for the atomic numbering. [b] Reference 22.

the basis of the isotope shift of the band. In this section, we first try to assign the vibrational bands due to the benzonitrile moiety of the ICT state of DMABN, by comparing the observed and calculated frequencies. We will also make reference to the established vibrational assignments of the ground-state DMABN.[52]

There is no experimental evidence on symmetry species of the Raman band at 1585 cm^{-1}. However, from its strong intensity, this band may be attributed to a totally symmetric (a_1) vibrational mode. Then, this Raman band is almost uniquely assigned to ν_{8a} of the benzene ring.

In both geometries for the calculation (planar or twisted), only ν_{19a} mode gives vibrational frequency around 1400 cm^{-1} among the a_1-symmetry species vibrational modes of benzonitrile moiety. The infrared band at 1425 cm^{-1} is hence undoubtedly assigned to ν_{19a} of the benzene ring.

The infrared band at 1220 cm^{-1} is attributed to a totally symmetric (a_1) vibration of the benzonitrile moiety, as is evident from the absence of isotope shift and the positive absorption peak. For the Raman band at 1182 cm^{-1}, we have again no clear evidence on symmetry species of the mode. However, the band is probably due to a totally symmetric (a_1) vibration, since the Raman intensity is moderately strong.[48] By comparing the observed vibrational frequencies with the calculated frequencies (Table 1) as well as the ground-state ones,[52] the infrared and Raman bands at 1220 and 1182 cm^{-1} may be assigned, respectively, to the ring C−CN stretch and ν_{9a} of the benzene ring. The frequencies of these modes are quite close to each other, and hence they may be easily hybridized. In that case the opposite assignment may be correct. Anyhow, totally symmetric vibrations of the benzonitrile moiety in this wavenumber region is practically limited to these two modes. The assignments of the Raman bands at 1585 and that of 1182 cm^{-1} are in accordance with those given by Kwok et al.[48]

For the Raman band observed at 946 cm^{-1}, Kwok et al. assigned it to an out-of-plane bending mode.[48] However, the Raman intensity seems to be a little too high as an out-of-plane band. If, as mentioned in the previous section, this band is due to the same mode as that giving rise to the infrared band at 959 cm^{-1}, the mode is obviously totally symmetric, from the positive sign of the absorption band. From comparison with the calculation, we presently consider that this mode is dominated by ν_{12} of the benzene ring, with sizable contributions from several other stretch, deformation, and C−H in-plane bending coordinates.

5.2. The Molecular and Electronic Structure of the ICT State. The observed vibrational frequency of the C−NMe_2 stretch (1276 cm^{-1} for the normal species) may indicate that this bond retains a single-bond character in the ICT state. In the PICT model, it is sometimes argued that the C−NMe_2 bond order is so increased that it possesses a double-bond character.[9,42]

TABLE 3: Vibrational Frequencies (in cm^{-1}) of Benzenoids, Quinoids, and the ICT State of DMABN

	benzenoids			quinoids		
mode[a]	toluene[b]	DMABN (S_0)[c]	tSB (S_1)[d]	BQM[e]	BQ[f]	DMABN (ICT)
8a	1605	1609	1533	1621	1663	1585
				1536	1613	
19a	1494	1529	1454	1344	1354	1425
8a−19a[g]	*111*	*80*	*79*	*277*	*309*	*160*
				192	*259*	
9a	1175	1180	1162	1173	1146	1182
C−NMe_2		1372				1276

[a] Wilson notation.[54] [b] Reference 56. [c] Reference 52. [d] S_1 State of *trans*-stilbene, ref 57. [e] *p*-Benzoquinodimethane, ref 55. Mode 8a of the ring is hybridized with the C=CH_2 stretch to give two modes at 1621 and 1536 cm^{-1}. [f] *p*-Benzoquinone, ref 55. Mode 8a of the ring is hybridized with the C=O stretch to give two modes at 1663 and 1513 cm^{-1}. [g] Difference between vibrational frequencies of 8a and 19a modes.

The present result may reject a strong double-bond character of the C−NMe_2 bond. However, it does not directly indicate that the CT state has a twisted structure. We have to analyze the experimentally obtained vibrational frequencies further in detail. In the following we first discuss quinoidal contribution to the CT state from the ring vibrational frequencies, and then compare the experimental data with the results of the CASSCF calculation.[22,49]

Vibrational frequencies of the ICT state of natural DMABN are compared with those of several representative benzenoid and quinoid compounds in Table 3. The ground state of DMABN is included in the table as a benzenoid molecule. Here we make use of the frequency difference between ν_{8a} and ν_{19a} as a measure of quinoidal character of the electronic and molecular structure. This idea may be qualitatively rationalized if we consider the atomic motions of the modes.[52] Both of these modes are totally symmetric C−C stretching of the benzene ring. In the ν_{8a} mode, stretching motions of C_2-C_3 and C_5-C_6 bonds have the most significant contribution, while in the ν_{19a} mode these coordinates have only very small or no contribution. When a molecule has a quinoidal structure, the C_2-C_3 and C_5-C_6 bonds would have double-bond characters whereas the other C−C bonds in the ring would have single-bond characters. Then, $\nu_{8a} - \nu_{19a}$ frequency difference of a quinoidal molecule would be much larger than that of a benzenoid molecule.

Now we compare the ν_{8a} and ν_{19a} frequencies of the ICT state of DMABN with those of other molecular species. The frequency difference between ν_{8a} and ν_{19a} for the ICT state is substantially larger than that for the ground state. That is, the ν_{8a} frequency of the ICT state is approximately similar to that of the ground state, whereas a serious low-frequency shift on going from the ground state to the ICT state is found for ν_{19a}. The observed frequency difference between the two modes is ∼80 cm^{-1} for the ground state[52] and ∼160 cm^{-1} for the ICT state. The frequency difference may not deviate considerably from 100 cm^{-1} for the benzenoids in Table 3, although it depends, of course, on the molecular species to some extent. In quinoid molecules represented by X=C_6H_4=X (ground state) where X is CH_2 or O, ν_{8a} is hybridized with C=X stretch to give two relatively high-frequency modes in the region of 1670−1530 cm^{-1}, while ν_{19a} appears at quite a low frequency around 1350 cm^{-1}.[55] Then, the frequency difference between ν_{8a} and ν_{19a} reaches even to 200−300 cm^{-1}. The observed frequency difference between ν_{8a} and ν_{19a} for the ICT state of DMABN is much larger than that for benzenoids, and smaller than that for quinoid molecules. This result suggests that both benzenoid and

quinoid electronic structures contribute to the ICT state of DMABN. The ICT state may be neither a pure benzenoid nor a pure quinoid. It is now worth checking the calculated bond lengths in Table 2 in relation to this discussion. In quinoid molecules in the ground electronic state,[55] the difference between bond lengths of C_1-C_2 (or C_3-C_4) and C_2-C_3 is around 0.1 Å, whereas in benzenoid molecules[52] the difference is mostly less than 0.03 Å. For the ICT state of DMABN, all the calculated bond lengths in Table 2 seem to show intermediate bond alteration between quinoid and benzenoid. On the other hand, as mentioned above, the $C-NMe_2$ stretch mode of the ICT state is observed in the single-bond stretch region, which suggests a benzenoid electronic structure. The electronic structure of the ICT state of DMABN is therefore supposed to be basically of benzenoid nature, with a significant contribution from quinoidal electronic structure.

Kummrow and co-workers recently performed vibrational analyses of the ground and excited states of DMABN and 4-aminobenzonitrile by CASSCF level calculations, and they compared the calculated $C\equiv N$ and $C-NMe_2$ stretch frequencies for some electronic states.[22,49] They have predicted the shift of $C-NMe_2$ stretch frequencies on going from the ground state to the ICT state assuming twisted and planar geometries, and have claimed that a final decision between PICT and TICT may be possible by comparing the calculated and observed shifts. According to their calculation, the $C-NMe_2$ stretch frequency in the TICT state is lower than that in the ground state, whereas that in the PICT state is higher. (This result is qualitatively consistent with an expectation that the $C-NMe_2$ bond order is lowered in the TICT and raised in the PICT.) Our experimental result is that the $C-NMe_2$ stretch frequency in the ICT state is lower than that in the ground state, which may lead to a conclusion that the ICT state has a twisted geometry, if we follow the logic given by Dreyer and Kummrow.[22] However, we must be sufficiently careful when we try to obtain the structural information by comparing observed and calculated intramolecular vibrational frequencies. It should be in general noticed that a single-bond stretch coordinate is always hybridized with other stretching and bending coordinates in a normal mode. It is difficult to discuss the bond-order change only from the frequency of the relevant stretching coordinate, unless contributions of other coordinates to the mode are sufficiently small. In the single-bond stretching region, this condition is usually not fulfilled. We consider that the frequency of the $C-NMe_2$ stretch may be one of parameters which reflects the molecular structure of the ICT state of DMABN but it is not possible to judge the structure only from this frequency.

Generally speaking, the CASSCF method adopted by Kummrow and co-workers surely gives more quantitative vibrational frequencies than the CIS method. However, the accuracy of the calculated frequencies should be judged by taking various types of vibrational modes into consideration, not by some specific modes. We consider that there are still difficulties in the results of CASSCF vibrational analysis on the CT excited state of DMABN, as mentioned in the following. The observed infrared band at 1425 cm^{-1} is assigned, from the isotope data, obviously to a mode without contribution from the methyl groups as discussed earlier. According to ref 49, however, the CASSCF calculation gives results not consistent with the experimental assignment (the band should be assigned to Me-group vibration if we follow ref 49). As for the observed b_2 vibrational band at 1276 cm^{-1}, there is no corresponding calculated vibrational mode in ref 49. For the observed strong band at 1220 cm^{-1}, it seems again difficult to explain by the CASSCF result of TICT structure.[49] From these considerations, it becomes clear that one should be very careful to make quantitative comparison between the observed vibrational frequencies and the calculated ones (in refs 22 and 49). In particular, small alteration in cross term force constants often cause large change of normal frequencies in the fingerprint region (the frequency changes sometimes reach even to ~100 cm^{-1}). The accuracy of the calculated frequencies should be sufficiently examined in order to discuss the structure of the CT state. A final decision may be possible only when the observed vibrational frequencies are compared with the calculated ones both for the dimethylamino group and for the benzonitrile moiety simultaneously. Dependence of the calculated vibrational frequencies on the basis set and the definition of active space (in CASSCF method) should be also examined.

In conclusion, we have established in the present study the assignments of the most of the observed transient vibrational bands of the ICT state of DMABN. The $C-NMe_2$ bond retains the single-bond character in the ICT state. The ring moiety is considered to have primarily an electronic structure of the benzenoid type, with a considerable contribution from the quinoidal electronic structure. Unfortunately, it is difficult in the present stage to conclude the geometric structure of the ICT state from the data obtained. Detailed vibrational analysis based on a more advanced theoretical treatment and measurements on other isotope-substituted samples (especially in the benzene ring) are desired in the future. If we can record (and assign) vibrational bands of methyl deformation and/or some other related modes and their polarization characteristics, it may also give valuable information on the structure.

Acknowledgment. This research was supported by Grants-in-Aid (Nos. 09640597 and 11440171) from the Ministry of Education, Science, Sports and Culture, and by a grant from the Morino Foundation for Molecular Science to H.O.

References and Notes

(1) Lippert, E.; Lüder, W.; Moll, F.; Nägele, W.; Boos, H.; Prigge, H.; Seibold-Blankenstein, I. *Angew. Chem.* **1961**, *73*, 685.
(2) Nakashima, N.; Mataga, N. *Bull. Chem. Soc. Jpn.* **1973**, *46*, 3016.
(3) Rotkiewicz, K.; Grellmann, K. H.; Grabowski, Z. R. *Chem. Phys. Lett.* **1973**, *19*, 315.
(4) Siemiarczuk, A.; Grabowski, Z. R.; Krówczyński, A.; Asher, M.; Ottolenghi, M. *Chem. Phys. Lett.* **1977**, *51*, 315.
(5) Grabowski, Z. R.; Rotkiewicz, K.; Siemiarczuk, A.; Cowley, D. J.; Baumann, W. *Nouv. J. Chim.* **1979**, *3*, 443.
(6) Rettig, W. *Angew. Chem., Int. Ed. Engl.* **1986**, *25*, 971.
(7) Lippert, E.; Rettig, W.; Bonačić-Koutecký, V.; Heisel, F.; Miehé, J. A. *Adv. Chem. Phys.* **1987**, *68*, 1.
(8) von der Haar, T.; Hebecker, A.; Il'ichev, Y.; Jiang, Y.-B.; Kühnle, W.; Zachariasse, K. A. *Recl. Trav. Chim. Pays-Bas* **1995**, *114*, 430.
(9) Zachariasse, K. A.; Grobys, M.; von der Haar, T.; Hebecker, A.; Il'ichev, Y. V.; Jiang, Y.-B.; Morawski, O.; Kühnle, W. *J. Photochem. Photobiol. A* **1996**, *102*, 59.
(10) Zachariasse, K. A.; Grobys, M.; von der Haar, T.; Hebecker, A.; Il'ichev, Y. V.; Morawski, O.; Rückert, I.; Kühnle, W. *J. Photochem. Photobiol. A* **1997**, *105*, 373.
(11) Il'ichev, Y. V.; Kühnle, W.; Zachariasse, K. A. *J. Phys. Chem. A* **1998**, *102*, 5670.
(12) Kato, S.; Amatatsu, Y. *J. Chem. Phys.* **1990**, *92*, 7241.
(13) Schuddeboom, W.; Jonker, S. A.; Warman, J. M.; Leinhos, U.; Kühnle, W.; Zachariasse, K. A. *J. Phys. Chem.* **1992**, *96*, 10809.
(14) Hayashi, H.; Ando, K.; Kato, S. *J. Phys. Chem.* **1995**, *99*, 955.
(15) Serrano-Andrés, L.; Merchán, M.; Roos, B. O.; Lindh, R. *J. Am. Chem. Soc.* **1995**, *117*, 3189.
(16) Sobolewski, A. L.; Domcke, W. *Chem. Phys. Lett.* **1996**, *250*, 428.
(17) Gedeck, P.; Schneider, S. *J. Photochem. Photobiol. A* **1997**, *105*, 165.
(18) Parusel, A. B. J.; Köhler, G.; Grimme, S. *J. Phys. Chem. A* **1998**, *102*, 6297.
(19) Sobolewski, A. L.; Sudholt, W.; Domcke, W. *J. Phys. Chem. A* **1998**, *102*, 2716.

(20) Sudholt, W.; Sobolewski, A. L.; Domcke, W. *Chem. Phys.* **1999**, *240*, 9.
(21) Chudoba, C.; Kummrow, A.; Dreyer, J.; Stenger, J.; Nibbering, E. T. J.; Elsaesser, T.; Zachariasse, K. A. *Chem. Phys. Lett.* **1999**, *309*, 357.
(22) Dreyer J.; Kummrow A. *J. Am. Chem. Soc.* **2000**, *122*, 2577.
(23) Rettig, W.; Bliss, B.; Dirnberger K. *Chem. Phys. Lett.* **1999**, *305*, 8.
(24) Zachariasse K. A. *Chem. Phys. Lett.* **2000**, *320*, 8.
(25) Wang, Y.; McAuliffe, M.; Novak, F.; Eisenthal, K. B. *J. Phys. Chem.* **1981**, *85*, 3737.
(26) Huppert, D.; Rand, S. D.; Rentzepis, P. M.; Barbara, P. F.; Struve, W. S.; Grabowski, Z. R. *J. Chem. Phys.* **1981**, *75*, 5714.
(27) Wang, Y.; Eisenthal, K. B. *J. Chem. Phys.* **1982**, *77*, 6076.
(28) Hicks, J.; Vandersall, M.; Babarogic, Z.; Eisenthal, K. B. *Chem. Phys. Lett.* **1985**, *116*, 18.
(29) Heisel, F.; Miehé, J. A. *Chem. Phys. Lett.* **1986**, *128*, 323.
(30) Okada, T.; Mataga, N.; Baumann, W. *J. Phys. Chem.* **1987**, *91*, 760.
(31) Meech, S. R.; Phillips, D. *J. Chem. Soc., Faraday Trans. 2* **1987**, *83*, 1941.
(32) Su, S.-G.; Simon, J. D. *J. Phys. Chem.* **1989**, *93*, 753.
(33) Weisenborn, P. C. M.; Huizer, A. H.; Varma, C. A. G. O. *Chem. Phys.* **1989**, *133*, 437.
(34) Leinhos, U.; Kühnle, W.; Zachariasse, K. A. *J. Phys. Chem.* **1991**, *95*, 2013.
(35) Kajimoto, O.; Nayuki, T.; Kobayashi, T. *Chem. Phys. Lett.* **1993**, *209*, 357.
(36) Fisz, J. J.; van Hoek, A. *Chem. Phys. Lett.* **1997**, *270*, 432.
(37) Hashimoto, M.; Hamaguchi, H. *J. Phys. Chem.* **1995**, *99*, 7875.
(38) Kobayashi, T.; Futakami, M.; Kajimoto, O. *Chem. Phys. Lett.* **1986**, *130*, 63.
(39) Peng, L. W.; Dantus, M.; Zewail, A. H.; Kemnitz, K.; Hicks, J. M.; Eisenthal, K. B. *J. Phys. Chem.* **1987**, *91*, 6162.
(40) Gibson, E. M.; Jones, A. C.; Phillips, D. *Chem. Phys. Lett.* **1987**, *136*, 454.
(41) Kobayashi, T.; Futakami, M.; Kajimoto, O. *Chem. Phys. Lett.* **1987**, *141*, 450.
(42) Warren, J. A.; Bernstein, E. R.; Seeman, J. I. *J. Chem. Phys.* **1988**, *88*, 871.
(43) Kajimoto, O.; Futakami, M.; Kobayashi, T.; Yamasaki, K. *J. Phys. Chem.* **1988**, *92*, 1347.
(44) August, J.; Palmer, F.; Simons, J. P.; Jouvet, C.; Rettig, W. *Chem. Phys. Lett.* **1988**, *145*, 273.
(45) Grassian, V. H.; Warren, J. A.; Bernstein, E. R.; Secor, H. V. *J. Chem. Phys.* **1989**, *90*, 3994.
(46) Howell, R.; Phillips, D.; Petek, H.; Yoshihara, K. *Chem. Phys.* **1994**, *188*, 303.
(47) Okamoto, H. *J. Phys. Chem. A* **2000**, *104*, 4182.
(48) Kwok, W. M.; Ma, C.; Phillips, D.; Matousek, P.; Parker, A. W.; Towrie, M. *J. Phys. Chem. A* **2000**, *104*, 4188.
(49) Kummrow, A.; Dreyer, J.; Chudoba, C.; Stenger, J.; Nibbering, E. T. J.; Elsaesser, T. *J. Chin. Chem. Soc.* **2000**, *47*, 721.
(50) Okamoto, H.; Tasumi, M. *Chem. Phys. Lett.* **1996**, *256*, 502.
(51) Okamoto, H. *Chem. Phys. Lett.* **1998**, *283*, 33.
(52) Okamoto, H.; Inishi, H.; Nakamura, Y.; Kohtani, S.; Nakagaki, R. *Chem. Phys.* **2000**, *260*, 193.
(53) Frisch, M. J.; Trucks, G. W.; Schlegel, H. B.; Scuseria, G. E.; Robb, M. A.; Cheeseman, J. R.; Zakrzewski, V. G.; Montgomery, J. A., Jr.; Stratmann, R. E.; Burant, J. C.; Dapprich, S.; Millam, J. M.; Daniels, A. D.; Kudin, K. N.; Strain, M. C.; Farkas, O.; Tomasi, J.; Barone, V.; Cossi, M.; Cammi, R.; Mennucci, B.; Pomelli, C.; Adamo, C.; Clifford, S.; Ochterski, J.; Petersson, G. A.; Ayala, P. Y.; Cui, Q.; Morokuma, K.; Malick, D. K.; Rabuck, A. D.; Raghavachari, K.; Foresman, J. B.; Cioslowski, J.; Ortiz, J. V.; Baboul, A. G.; Stefanov, B. B.; Liu, G.; Liashenko, A.; Piskorz, P.; Komaromi, I.; Gomperts, R.; Martin, R. L.; Fox, D. J.; Keith, T.; Al-Laham, M. A.; Peng, C. Y.; Nanayakkara, A.; Gonzalez, C.; Challacombe, M.; Gill, P. M. W.; Johnson, B.; Chen, W.; Wong, M. W.; Andres, J. L.; Gonzalez, C.; Head-Gordon, M.; Replogle, E. S.; Pople, J. A. *Gaussian 98 (Revision A.7)*; Gaussian, Inc.; Pittsburgh, PA, 1998.
(54) Wilson, E. B., Jr. *Phys. Rev.* **1934**, *45*, 706.
(55) Yamakita, Y.; Tasumi, M. *J. Phys. Chem.* **1995**, *99*, 8524.
(56) Tasumi, M.; Urano, T.; Nakata, M. *J. Mol. Struct.* **1986**, *146*, 383.
(57) Urano, T.; Hamaguchi, H.; Tasumi, M.; Yamanouchi, K.; Tsuchiya, S.; Gustafson, T. *J. Chem. Phys.* **1989**, *91*, 3884.